

Dynamic spin-lattice coupling and nematic fluctuations in NaFeAs

Yu Li,¹ Zahra Yamani,² Yu Song,¹ Weiyi Wang,¹ Chenglin Zhang,¹ David W. Tam,¹ Tong Chen,¹ Ding Hu,^{1,3} Zhuang Xu,³ Songxue Chi,⁴ Ke Xia,^{3,5} Li Zhang,³ Shifeng Cui,³ Wenan Guo,³ Ziming Fang,³ Yi Liu,³ and Pengcheng Dai^{1,3,*}

¹*Department of Physics and Astronomy, Rice University, Houston, Texas 77005, USA*

²*Canadian Nuclear Laboratories, Chalk River Laboratories, Chalk River, Ontario K0J 1J0, Canada*

³*Center for Advanced Quantum Studies and Department of Physics, Beijing Normal University, Beijing 100875, China*

⁴*Quantum Condensed Matter Division, Oak Ridge National Laboratory, Oak Ridge, Tennessee 37831, USA*

⁵*Synergetic Innovation Center for Quantum Effects and Applications (SICQEA), Hunan Normal University, Changsha 410081, China*

(Dated: May 10, 2018)

We use inelastic neutron scattering to study acoustic phonons and spin excitations in single crystals of NaFeAs, a parent compound of iron pnictide superconductors. NaFeAs exhibits a tetragonal-to-orthorhombic structural transition at $T_s \approx 58$ K and a collinear antiferromagnetic (AF) order at $T_N \approx 45$ K. While longitudinal and out-of-plane transverse acoustic phonons behave as expected, the in-plane transverse acoustic phonons reveal considerable softening on cooling to T_s , and then harden on approaching T_N before saturating below T_N . In addition, we find that spin-spin correlation lengths of low-energy magnetic excitations within the FeAs layer and along the c -axis increase dramatically below T_s , and show weak anomaly across T_N . These results suggest that the electronic nematic phase present in the paramagnetic tetragonal phase is closely associated with dynamic spin-lattice coupling, possibly arising from the one-phonon-two-magnon mechanism.

INTRODUCTION

Spin waves (excitations) and phonons are two fundamental quasiparticles in a solid describing propagating disturbance of the ordered magnetic moment and lattice vibrations, respectively [1]. They are the byproducts of linearized theories that ignore all the higher-order terms than quadratic term and neglect quasiparticle-quasiparticle interactions [2] unlikely interacting with each other [3]. However, in systems with multiple coupled degrees of freedom, the interaction affects the self energy of the quasiparticles and changes their intrinsic dispersion relationship. Therefore, discovering and understanding how the interaction and coupling changes the spectra of spin excitations and phonons and further influences the electronic properties of solids are one of the most important themes in modern condensed matter physics.

In general, spin-lattice (magnon-phonon) coupling can modify the spin excitations in two different ways. First, the static lattice distortion coupled with magnetic order, as seen in some parent compounds of iron-based superconductors [4, 5], can dramatically change the effective magnetic exchange anisotropy in a near square lattice of the antiferromagnetic (AF) ordered phase [6]. Second, the dynamic lattice vibrations (phonons) interacting with time-dependent spin excitations may create energy gaps in the magnon dispersion at the nominal intersections of the magnon and phonon modes [1], as seen in insulating non-collinear antiferromagnet (Y,Lu)MnO₃ [7]. Similarly, spin waves can hybridize with optical phonon modes near the zone boundary and form broadened magnon-phonon excitations in metallic ferromagnetic manganites [8]. In both cases, magnon-phonon interactions only form hybridized excitations at the magnon phonon intersection points due to the repulsive magnon-phonon dispersion curves.

In this paper, we report a different form of magnon-phonon interaction in NaFeAs, which is a parent compound of iron pnictide superconductor and exhibits a tetragonal-to-orthorhombic structural transition at $T_s \approx 58$ K followed by a collinear AF order at $T_N \approx 45$ K [Fig. 1(a)] [9–12]. For temperatures between T_N and T_s , NaFeAs has an electronic nematic phase, a form of electronic order which breaks the rotational symmetries without changing the translational symmetry of the underlying lattice [13–26], which may play an important role in high temperature superconductivity [27, 28]. Instead of the usual magnon-phonon interaction where the magnon dispersion would intersect with the phonon dispersion in reciprocal space, we find evidence for magnon-phonon interaction in NaFeAs, where the low-energy acoustic phonons near the nuclear zone center Γ point in NaFeAs can interact with the low-energy spin excitations near the AF zone center M point at \mathbf{Q}_{AF} in reciprocal space without direct phonon-spin excitation crossing [Fig. 1(b) and 1(c), Figs. 2-5]. Since both the in-plane transverse acoustic (IPTA) phonons [Fig. 1(b)] and spin excitations show dramatic anomaly across T_s , our results indicate that the magnon-phonon interaction may be responsible for the low-temperature electronic nematic phase in NaFeAs [13–26]. Although not conclusively established, one possible microscopic interpretation of these results is the one-phonon-two-magnon scattering mechanism [29, 30]. By

considering dynamical spin exchange coupling tuned by local lattice vibration, we calculate the effect of magnon-phonon coupling in one-dimensional (1D) spin chain. Further phonon dispersion calculations using density function theory (DFT) on NaFeAs demonstrates that softening of the IPTA mode occurs at $q \rightarrow 0$ in the presence of stripe type AF spin-spin correlations, consistent with our observation. Therefore, instead of a pure spin [14–17] or lattice (orbital) [31–36] degree of freedom, dynamic spin-lattice coupling is important for the electronic nematic phase and anisotropic electronic properties in the paramagnetic state of NaFeAs.

RESULTS

Neutron Scattering

We chose to study NaFeAs because transport [18, 19], angle resolved photoemission spectroscopy (ARPES) [20, 21], scanning tunneling microscopy [22, 23], and neutron scattering experiments [24–26] provided ample evidence for the presence of an electronic nematic phase in $T_N \leq T \leq T_s$. By assuming weak spin-orbit and spin-lattice coupling, most theoretical understandings of the nematic phase involve pure “spin” or “orbital” degrees of freedom. In the first case, the electronic nematic phase originates from spin fluctuations which couple quadratically to the nematicity but have no direct coupling to lattice [14–16]. Here, key predictions of the theory, such as the enhanced spin excitation intensity and correlation length at the AF ordering wave vector \mathbf{Q}_{AF} in the paramagnetic phase of iron pnictides [37, 38], have been confirmed by inelastic neutron scattering experiments [24–26]. Alternatively, ferro-orbital order or orbital fluctuations [31–36], seen in ARPES measurements as a pronounced energy splitting of bands with d_{xz} and d_{yz} orbital characters above T_N [20, 21], may induce the electronic nematicity through the direct ferro-orbital order (fluctuations) and orthorhombic lattice distortion (or vibration) coupling [39, 40].

The difficulty in sorting out the microscopic origin of the nematic phase in iron pnictides lies in the fact that the relevant degrees of freedom, such as spin, lattice, and orbital are closely entangled [39, 40]. However, DFT calculations of iron pnictides [41–43] shows a remarkable sensitivity of superconductivity and magnetism to the lattice, particularly the iron pnictogen height, thus suggesting a strong dynamic spin-lattice coupling in this system. Measurements and calculations on the phonon dispersions in CaFe_2As_2 and BaFe_2As_2 suggest that magnetism must be taken into account when calculating the phonon frequencies and phonons are strongly coupled not to the static AF order, but to spin fluctuations [44–46]. In addition, inelastic X-ray and neutron scattering measurements on AF ordered BaFe_2As_2 and SrFe_2As_2 where $T_N \approx T_s$ show a softening of the IPTA phonon on cooling to T_s [Fig. 1(a) and 1(b)], followed by a dramatic hardening below T_N/T_s [47, 48]. For electron-doped superconducting $\text{Ba}(\text{Fe}_{1-x}\text{Co}_x)_2\text{As}_2$ with $T_c < T_N < T_s$, the softening of the IPTA phonon stops at T_s on cooling, and the hardening of the mode passes through T_N unabated before softening again below T_c [49]. On the other hand, a sharp enhancement in the in-plane spin-spin correlation length was found below T_s at \mathbf{Q}_{AF} in LaFeAsO and $\text{Ba}(\text{Fe}_{1-x}\text{Co}_x)_2\text{As}_2$ [25], suggesting a strong feedback effect of the structural transition and nematic order on the low-energy spin fluctuations. Although these results suggest a correlation between the evolution of the transverse acoustic phonon and low-energy spin fluctuations, the measurements were carried out on different samples by different groups, thus making it difficult to establish a direct connection between lattice vibrations and spin fluctuations.

To resolve this problem, we use inelastic neutron scattering to study phonons and spin excitations in single crystals of NaFeAs, which is the parent compound of $\text{NaFe}_{1-x}\text{Co}_x\text{As}$ family of iron-based superconductors [50]. Our measurements were carried out on the C5 triple-axis spectrometer at the Canadian Neutron Beam center, Chalk River Laboratories, with a fixed final neutron energies of $E_f=8.04$ meV and 14.56 meV for phonon measurements and $E_f=13.7$ meV for spin fluctuation measurements. Some scans of the IPTA phonon were carried on the HB-3 triple-axis spectrometer at the High Flux Isotope Reactor (HFIR), Oak Ridge National Laboratory, with $E_f=14.7$ meV. The wave vector transfer \mathbf{Q} in three-dimensional (3D) reciprocal space in \AA^{-1} is defined as $\mathbf{Q} = H\mathbf{a}^* + K\mathbf{b}^* + L\mathbf{c}^*$, with $\mathbf{a}^* = \frac{2\pi}{a}\hat{\mathbf{a}}$, $\mathbf{b}^* = \frac{2\pi}{b}\hat{\mathbf{b}}$ and $\mathbf{c}^* = \frac{2\pi}{c}\hat{\mathbf{c}}$, where H , K and L are Miller indices. In the paramagnetic tetragonal state, we have $a = b = a_T = b_T = 3.93$ \AA and $c = 6.98$ \AA [Fig. 1(a)]. In the AF ordered phase, $a_o \approx b_o \approx \sqrt{2}a$ \AA [Figs. 1(b) and 1(c)] and AF spin fluctuations occur at $\mathbf{Q}_{\text{AF}} \approx (0.5, 0.5)$ [4]. The phonon measurements were made on a single piece of NaFeAs single crystal weighing ~ 2.5 g with mosaic $< 1^\circ$ aligned in the $[H, K, 0]$ and $[H, 0, L]$ scattering planes [Fig. 1(c)]. The spin fluctuation measurements were carried out using a well aligned pack of single crystals (~ 10 g) with mosaic $< 3^\circ$ aligned in the $[H, H, L]$ scattering plane [Fig. 3(a)].

To measure IPTA, out-of-plane transverse acoustic (OPTA) and longitudinal acoustic (LA) phonon modes in NaFeAs, we probed wave vectors $\mathbf{Q} = (q, 2, 0)$, $(q, 0, 5)$, and $(2+q, 0, 0)$, respectively, where \mathbf{q} is the reduced momentum transfer away from the Γ point in reciprocal space [Fig. 1(c)] [47, 48]. In the long wave length (small $|\mathbf{q}|$) limit, one would expect linear dispersions for acoustic phonons $E = vq$, where E is the energy of the mode and v is the sound

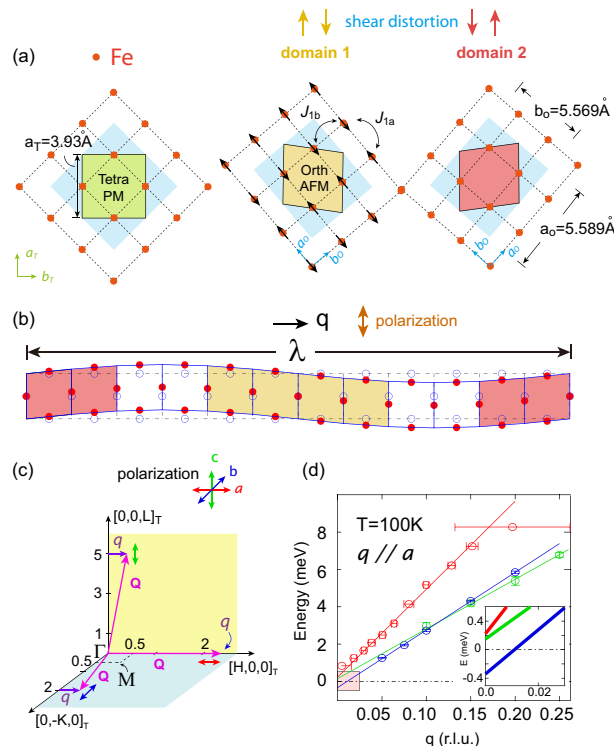


FIG. 1: (Color online) (a) Left: schematics of the Fe layers in NaFeAs. Red spots represent Fe atoms and the tetragonal (orthorhombic) unit cell is shown in green (blue) shaded square. Middle and right panels are the two orthorhombic domains. The yellow and red area are the tetragonal unit cells with opposite shear distortions. The arrows in the middle panel indicates spin direction in the AF ordered phase. The orthorhombic lattice parameters are $a_o = 5.589 \text{ \AA}$ and $b_o = 5.569 \text{ \AA}$. (b) A particular IPTA phonon mode with a momentum propagating horizontally to the right but with Fe atoms oscillating vertically. λ , the size of the probing domain, is inversely related to q . (c) The three different equivalent positions in reciprocal space used in our neutron scattering measurements in order to determine all three acoustic phonon branches. The purple arrows with q are the momentum of the measured phonons along the $[H, 0, 0]$ direction and the double-headed arrows represent the phonon polarizations along the a (red, LA), b (blue, IPTA) and c (green, OPTA) axis. (d) The corresponding dispersions of the three phonon modes at 100 K estimated from data in [51]. The inset shows expanded view of the low-energy part of the dispersion.

velocity. Figure 1(d) shows our measured dispersions of LA, OPTA, and IPTA acoustic phonon modes at 100 K [51]. While LA and OPTA phonons behave as expected and passed through the zero energy at $q = 0$, the IPTA mode, which corresponds to the $q = 0$ shear modulus mode C_{66} seen in the ultra sound spectroscopy measurements [52–54], has a lower sound velocity as $q \rightarrow 0$ [dashed lines in Fig.2(a)]. The solid lines are linear fits to the large wave vector data.

Figure 2(a) shows dispersions of the IPTA phonons determined from a series of constant- \mathbf{Q} scans at different temperatures [51]. While the high- q (> 0.2 r.l.u.) part of the dispersion hardens slightly with decreasing temperature due to stiffer lattice at low temperature (but showed no anomaly across T_s and T_N), the low- q (< 0.2 r.l.u.) part of the dispersion is strongly temperature dependent [Fig. 2(b)] [51]. This is seen in the temperature dependence of the constant- \mathbf{Q} scans at $q = 0.05$ r.l.u. [Fig. 2(c)], where the peak center shifts from 1.25 meV at 100 K to 0.9 meV at 60 K near T_s . On further cooling to below T_s , the phonon hardens with decreasing temperature. The temperature dependence of the phonon energy at different q is summarized Figs. 2(d) and 2(e).

In general, acoustic phonons with different polarizations should exhibit similar linear dispersion dependence at similar temperatures. When phonons couple with electrons or other elementary excitations, their peak position, width, and intensity might change [55]. While LA and OPTA phonon dispersions in Fig. 1(d) follow $E = vq$ below $q \leq 0.2$ r.l.u., IPTA phonon dispersion is $E = vq + b$ with $b < 0$ [Fig. 1(d)]. Since IPTA phonon at $q = 0.2$ r.l.u. is weakly temperature dependent [Fig. 2(a) and 2(b)], its temperature dependent effect for $q < 0.2$ r.l.u. will be absorbed into the parameter b [Fig. 2(a)] [51]. Figure 2(f) shows temperature dependence of b for the LA, OPTA, and IPTA phonons obtained by fitting with $E = vq + b$. While the LA and OPTA phonons behave as expected with $b = 0$, the values of b for the IPTA mode are negative in both the AF ordered and paramagnetic state, thus suggesting the presence of the IPTA phonon-elementary excitation (either spin or orbital) coupling that is independent of the

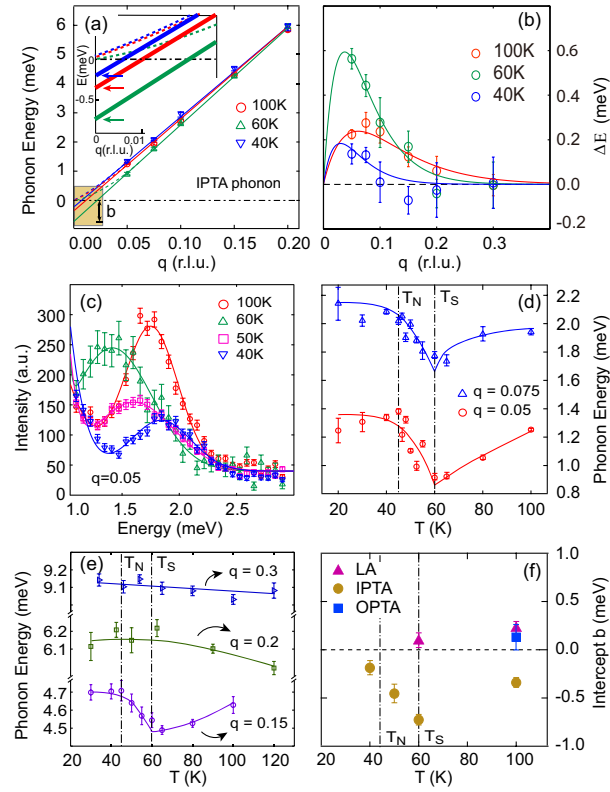


FIG. 2: (Color online) (a) Temperature dependence of the phonon dispersions of the IPTA mode near the zone center at 100 K, 60 K, and 40 K. The inset shows the expanded view of the low-energy part of the dispersions. (b) The estimated amplitude of the softening of the IPTA phonons at difference temperatures obtained by subtracting an assumed linear dispersion $E = vq$. The solid lines are guides to the eye. (c) Temperature dependence of constant- q scans at $q = 0.05$ for the IPTA mode. (d) and (e) Temperature dependence of the phonon energy measured at $q = 0.05, 0.075$ and $0.1, 0.15$, respectively. The phonon softening on cooling to T_s is observed at $q = 0.05, 0.075$, and 0.15 rlu but absent at $q = 0.20$ and 0.3 rlu. The phonon hardening below T_s are seen for wave vectors below $q = 0.2$ r.l.u. (f) Temperature dependence of the intercept b estimated for all three acoustic branches shown in Fig. 1(d).

magnetic ordering. Since such coupling is absent for the LA and OPTA phonon modes, we conclude that the nonlinear dispersion curves seen in the IPTA phonon mode at small q and their strong temperature dependence around T_s are due to the IPTA phonon and elementary (spin or orbital) excitation coupling with the absolute value b reflecting the coupling strength.

In addition to phonons, spin fluctuations are another important elementary excitations in iron pnictides [4, 13]. Distinct from acoustic phonons which are observed near nuclear Bragg peak positions such as $(2, 0, 0)$, low-energy spin fluctuations in NaFeAs occur near the $\mathbf{Q}_{\text{AF}} = (0.5, 0.5, 0.5)$ AF zone center in reciprocal space [Fig. 3(a)] [4]. Figure 3 summarizes temperature dependence of the in-plane spin-spin correlations for spin fluctuations with energies of $E = 3$ meV, 5 meV, and 8 meV along the cut 1 and cut 2 directions as shown in Fig. 3(a). Figure 3(b-e) shows temperature dependence of the line width and the corresponding spin correlation length ξ , respectively. A sharp reduction in the peak linewidth and a dramatic increase in the spin-spin correlation lengths are seen below T_s [51]. They are accompanied by the increase of the intensities at the peak centers, reflecting a redistribution of the magnetic spectral weight in the nematic phase. While these results are somewhat different from a neutron scattering work on NaFeAs [56], which finds no dramatic anomaly across T_s , they are consistent with previous work on LaFeAsO and $\text{Ba}(\text{Fe}_{0.953}\text{Co}_{0.047})_2\text{As}_2$, which was interpreted as resulting from the long-range nematic order below T_s [25]. We note that a phonon at $q = 0.05$ probes coherent lattice vibrations of ~ 20 unit cells, giving a dynamic length scale of ~ 40 - 80 Å. These values are similar to the observed spin-spin correlation lengths above T_s , suggesting that correlated spin domains might be limited by sizes of the dynamic structural domains.

To further understand spin excitations across T_s , we carefully studied temperature dependence of spin-spin correlations along the c -axis. Figures 4(a)-(d) are the background subtracted wave vector scans along the $[0.5, 0.5, L]$ direction at spin excitation energy of $E = 2$ meV and different temperatures. At $T = 60$ K ($> T_s$), the scattering is

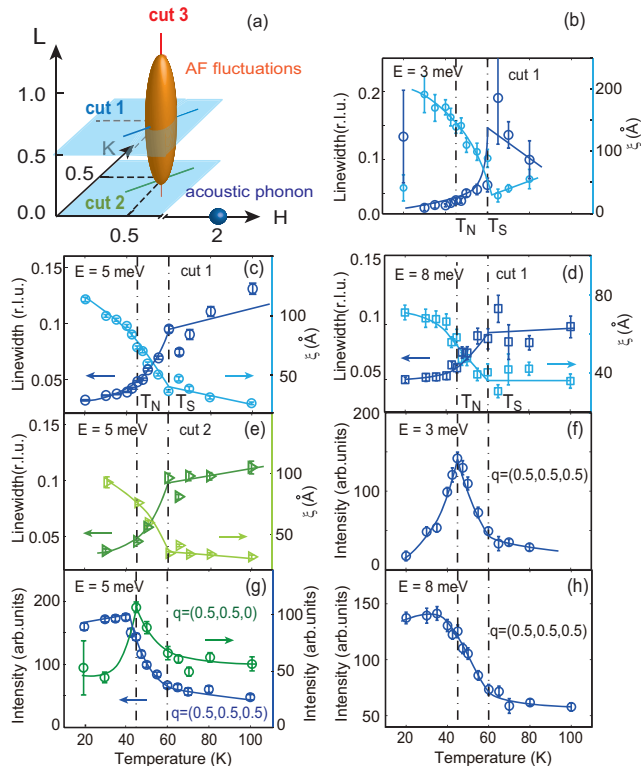


FIG. 3: (Color online) (a) Sketch of the reciprocal space in which AF spin fluctuations and acoustic phonons are marked as yellow ellipsoid and blue sphere. The directions along which we measured in the experiment are shown as blue, green and red lines. (b-e) Temperature dependent line widths and correlation lengths of the low energy spin fluctuations. They are measured along the cut 1 direction at (b) 3 meV, (c) 5 meV, (d) and 8 meV, (e) along the cut 2 direction at 5 meV. (f-h) Temperature dependence of the peak intensity in each scan. It is clear that there are negative correlations between the peak intensity and the peak width before the system enters into the AF ordered state, representing a redistribution of spectral weight in the nematic phase below T_s . The vertical dashed lines mark the magnetic and structural transition temperatures.

essentially featureless and decreases with increasing L due to the iron magnetic form factor, suggesting that magnetic excitations are two-dimensional (2D) rods along the c -axis in reciprocal space [Fig. 4(d)]. On cooling to $T = 55$ K ($< T_s$), Two broad peaks emerge around $L = \pm 0.5$ rlu indicating increased c -axis spin-spin correlation [Fig. 4(c)]. Upon further cooling to $T = 50$ K and 45 K ($> T_N$), these peaks become progressively better established [Fig. 4(b) and 4(a)]. The solid lines of Fig. 4(a)-(d) are fits to these peaks with a periodic Lorentzian function [51]. Figures 4(e)-(g) plot temperature dependence of the fitted width and corresponding spin correlation length at $E = 2$ meV, 3 meV, and 5 meV. Inspection of the Figures reveals a clear change of the c -axis spin correlation length below T_s , suggesting that a spin fluctuation crossover from 2D to 3D occurs below T_s and above T_N . Figure 4(h) shows temperature dependence of the integrated intensities over the range from $L = -1$ to $L = 1$, which again reveal an clear increase in magnetic scattering below T_s . From results described in Figs. 3 and 4, we conclude that the low energy spin fluctuations in NaFeAs respond dramatically to the structural transition and change its spectral distribution below T_s .

Theoretical considerations and density functional theory calculation

Given the simultaneous occurrence of the dramatic increasing spin correlation length at \mathbf{Q}_{AF} and a hardening of the IPTA phonon at Γ point below T_s (Figs. 2-4), it is interesting to ask if the low-energy spin fluctuations are coupled to the IPTA phonons. To address this question, we consider the differences between paramagnetic tetragonal and orthorhombic phases. In the paramagnetic tetragonal phase, iron spins are completely random, spending equal amount of time along all directions. On cooling to paramagnetic orthorhombic phase below T_s , the direction of the spin alignment gets approximately fixed to the low-temperature AF ordered collinear phase due to dynamic spin-lattice coupling, so that within a structural domain iron spins in the nearest neighbors are predominantly anti-parallel

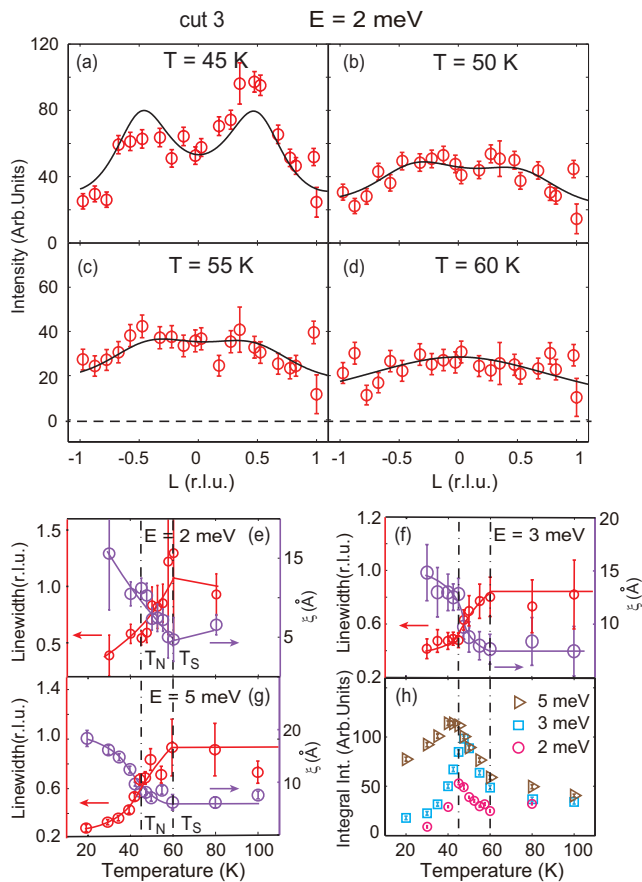


FIG. 4: (Color online) (a-d) Constant- E ($E = 2$ meV) scans along the cut 3 direction as shown in Fig. 3(a) at 45 K, 50 K, 55 K and 60 K. Background scans are obtained by measuring at $q = (0.4, 0.4, L)$ and $(0.6, 0.6, L)$ and subtracted from the raw data. The scan at 60 K is featureless. On cooling to 55 K, two weak peaks show up around $L = \pm 0.5$ rlu. Upon further cooling, these peaks become prominent at $T = 45$ K. They disappear below T_N due to the opening of a spin gap. The total magnetic scattering intensity increases on cooling. The solid lines are fits with periodic Lorentz function [51]. (e-g) Temperature dependence of the line widths and correlation lengths of the low energy spin fluctuations along the c -axis direction [cut 3 in Fig. 3(a)] at 2 meV, 3 meV, and 5 meV. (h) Temperature dependence of the integrated intensity along the cut 3 direction at different energies [51].

along the orthorhombic a_o axis and parallel along the b_o axis. As a consequence, the magnetic correlation length changes abruptly across T_s but does not become infinite due to the lack of long-range magnetic order. Regardless of a detailed microscopic spin-lattice coupling mechanism, this picture is valid and suggests a magnetic origin of the nematic phase [16].

To provide a possible microscopic description of the spin-lattice coupling, we consider the magnitude of the effective magnetic exchange couplings in NaFeAs. By fitting the spin wave spectra throughout the Brillouin zone at 5 K using a Heisenberg Hamiltonian, it was found that the effective magnetic exchange couplings along the orthorhombic a_o and b_o axes are $SJ_{1a} = 40 \pm 0.8$ meV and $SJ_{1b} = 16 \pm 0.6$ meV, respectively, where $S \approx 1$ is the spin of the system [57]. Since the distances between the nearest Fe-Fe neighbors in the AF orthorhombic phase are $a_o/2 = 2.795$ Å and $b_o/2 = 2.785$ Å [10], the large changes in the magnetic exchange in the AF ordered phase may arise from tiny differences in the in-plane Fe-Fe distances within the Heisenberg Hamiltonian [Fig. 5(a)] [58]. In the paramagnetic tetragonal state, the shear modulations of the IPTA phonon mode [Figs. 1(a) and 1(b)] may induce large changes in magnetic exchange through dynamic spin-lattice coupling [Fig. 5(b)]. In previous ultrafast optical spectroscopy measurements on $\text{Ba}(\text{Fe}_{1-x}\text{Co}_x)_2\text{As}_2$, it was found that coherent optical phonon motions of As atoms on ultrafast timescales induced by a femtosecond optical pulse can produce transient dynamic AF and/or nematic order at temperatures above T_s through possible modifications of the Fermi surfaces and dynamic spin-lattice coupling [59, 60]. For conventional AF insulator such as $(\text{Y,Lu})\text{MnO}_3$, the effect of dynamic spin-lattice coupling is to create energy gaps in the magnon dispersion at the nominal intersections of the magnon and phonon modes [7]. However, this cannot explain our

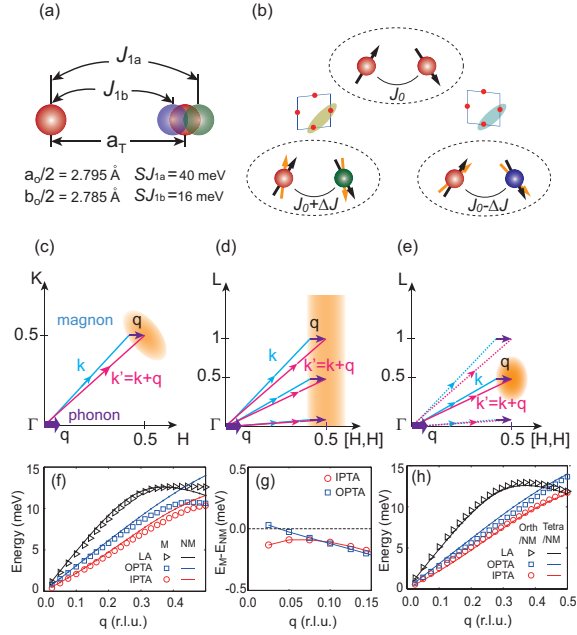


FIG. 5: (Color online) (a) Schematics of the nearest neighbor Fe-Fe bond. The small difference between $a_o/2$ and $b_o/2$ and the large difference between J_{1a} and J_{1b} renders a nonnegligible $\Delta J/\Delta r$, which entangles the lattice and magnetism. (b) One pair of magnetic Fe ions in the paramagnetic tetragonal phase with the magnetic binding energy of $E_b = J_0 S_1 S_2 \cos \theta$. As the Fe-Fe bond stretches, the spin exchange coupling increases and thus there is an energy transfer from the lattice to the spin system. (c) The scattering triangle required by the momentum conservation in the dynamic spin-lattice coupling process within the $[H, K]$ plane. (d) and (e) The momentum triangles in the $[H, H, L]$ plane above and below T_s . As spin fluctuations undergoes a 2D-to-3D transition, a large part of the spin-lattice coupling scattering channel would be blocked. (f) Comparison of the phonon dispersions obtained from DFT calculations with (markers, M) and without (solid lines, NM) magnetism assuming a tetragonal lattice. We note that nonmagnetic tetragonal phase does not really exist in NaFeAs since spin correlations are strong at temperatures far above T_N and T_s . (g) Wave vector dependence of $E_M - E_{NM}$ for IPTA and OPTA phonon modes. (h) Comparison of the phonon dispersions obtained from DFT calculations with nonmagnetic (NM) Fe site assuming orthorhombic (markers) and tetragonal (solid lines) lattice. The black, blue, and red color represents LA, OPTA, and IPTA phonon modes.

observation in NaFeAs, since the low-energy acoustic phonons and spin fluctuations are located at different wave vectors in reciprocal space [Fig. 3(a)].

To solve this problem, we consider the one-phonon-two-magnon scattering mechanism [29, 30]. Although such mechanism is no different from the usual magnetoelastic coupling or magnon-phonon coupling, it provides a simple pictorial way to visualize such coupling. Theoretically, it has been found that spin-lattice coupling due to the one-phonon-two-magnon scattering process in an antiferromagnet can affect the spin wave broadening/damping, dispersion, and intensity [61]. Since spin fluctuations in iron pnictides exhibit spin-wave-like features above T_N up to very high temperatures [62], such magnon-phonon coupling must also exist in the paramagnetic tetragonal phase. Figure 5(b) schematically illustrates how such a dynamic spin-lattice scattering mechanism might work. In the paramagnetic tetragonal phase with strong AF spin fluctuations, the neighboring spins are aligned anti-parallel on a time scale determined by the energy of the fluctuations and the average moment of the system at elastic position ($E = 0$ or infinite time) is still zero. When an IPTA phonon with momentum \mathbf{q} and energy E_0 is emitted near Γ point [Fig. 1(b)], the Fe-Fe distance stretches and thus the exchange coupling increases from J_0 to $J_0 + \Delta J$ [Fig. 5(b)] [51]. This represents an energy transfer from the lattice to the spin system, annihilating one phonon and producing spin fluctuations, and vice versa.

To test the possible spin-lattice coupling, we built a toy model of 1D spin chain in which the spin exchange coupling is tuned by the local lattice vibration induced by a passing phonon (see Ref. [51], section IV). Similar to the recent calculations on the effect of one-phonon-two-magnon to the indirect K -edge resonant inelastic x-ray scattering spectrum of a 2D Heisenberg antiferromagnet [61], we find that spin waves in 1D chain are also affected by the lattice distortion. In particular, the periodic lattice distortion affect spin waves, which in turn leads to the phonon softening at small q similar to our observation in NaFeAs (Fig. S21). Since analytical analysis in the 2D case is difficult, we performed DFT calculations to compare the phonon dispersions of NaFeAs with and without magnetic moment on the Fe site. The open triangles, squares, and circles in Figure 5(f) are DFT calculated LA, OPTA, and

IPTA phonon dispersions with Fe magnetic moment, respectively. The solid lines in the same figure show identical calculations without magnetism. While the main effect of magnetism is to soften the OPTA and IPTA phonons near the zone boundary ($q = 0.5$) consistent with earlier work [44–46], its effect on the low-energy OPTA and IPTA phonons can be seen by comparing phonon energies with magnetism (E_M) and without magnetism (E_{NM}). Figure 5(g) shows wave vector dependence of $E_M - E_{NM}$, revealing a clear difference between OPTA and IPTA phonons below $q = 0.075$. These calculations suggest that the presence of magnetic moment on Fe has much larger effect on the low energy IPTA phonons, consistent with our observation of the phonon softening determined by the intercept b [Fig. 2(b)]. To test if the small orthorhombic lattice distortion in the nematic phase of NaFeAs can affect acoustic phonons without magnetism, we show in Fig. 5(h) the calculated phonon dispersions in orthorhombic and tetragonal states in the nonmagnetic state. Within the errors of our calculation, we find no evidence of phonon softening due to lattice orthorhombicity. From these results, we conclude that the presence of magnetism and spin-spin correlations selectively influence the dispersion of the IPTA phonon at $q \rightarrow 0$.

DISCUSSION AND CONCLUSION

Assuming that the spin-lattice coupling in NaFeAs is due to the one-phonon-two-magnon mechanism, the scattering process must satisfy the energy and momentum conservation [30, 63]. Two magnons with momentum \mathbf{k} and \mathbf{k}' and energy E and E' with a relationship $\mathbf{q} = \mathbf{k} + \mathbf{k}'$ and $E_0 = E + E'$ (Positive E means generating and negative E means annihilating) must be introduced as shown in Fig. 5(c). The scattering amplitude is constrained by the momentum triangle and depends on the detail of the spin fluctuation dispersion [30]. In the paramagnetic tetragonal state, the magnetic scattering is a rod centered around $\mathbf{Q}_{AF} = (0.5, 0.5)$ in the FeAs plane [Figs. 3(a), 4(d), and 5(d)]. This implies a large phase space for the dynamic spin-lattice coupling to occur. However, when a 2D-to-3D crossover in spin fluctuations occurs below T_s , the spin-lattice coupling phase space is greatly reduced as shown in Fig. 5(e). Since the IPTA phonon mode dynamically changes the nearest neighbor Fe-Fe distance which is directly coupled to the nearest neighbor magnetic exchange coupling, the reduced scattering phase space below T_s explains the recovery of the phonon softening (*phonon hardening*) at low temperature in NaFeAs. Therefore, the observed IPTA phonon hardening below T_s is a sign of reduced phonon-magnon coupling induced by the 2D-to-3D spin fluctuation crossover. In this picture, the narrowing of the low-energy in-plane spin fluctuations below T_s is associated with the orthorhombic lattice distortion and nematic order, which increases the effective exchange coupling along a and therefore the spin wave velocity. Since finite magnetic exchange coupling along the c -axis is required to establish the eventual 3D AF long-range order, the presence of the quasi-2D spin fluctuations in the paramagnetic tetragonal phase and the resulting large dynamic spin-lattice coupling are directly associated with the observed nematic fluctuations in a variety of experiments [19–26]. The energy scale of the phonon softening ~ 1 meV [64] is consistent with the slow recovery of the nematic order on a timescale of several or decades of ps observed by time-resolved polarimetry [60], further confirming its close relationship with the nematic fluctuations.

Although the one-phonon-two-magnon mechanism described above may provide a pictorial way to explain the experimentally observed phonon and spin excitation anomaly across T_s in NaFeAs, we recognize that any effect of dynamic spin-lattice coupling can be described as such process, and we have not established a quantitative perturbative theory based on such process. Regardless the microscopic origin of the observed phonon and spin excitation anomaly across T_s , our experimental results revealed a clear coupling between low-energy acoustic phonon and spin excitations at T_s . Therefore, instead of the pure spin or lattice (with associated orbital ordering) as the driving force for the electronic nematic phase in iron pnictides, a strong dynamic spin-lattice-orbital coupling in the paramagnetic tetragonal phase is responsible for the observed electronic nematic order and anisotropic behavior.

ACKNOWLEDGMENTS

We thank Rong Yu and Qimiao Si for helpful discussions. The single crystal growth and neutron scattering work at Rice is supported by the U.S. DOE, BES under contract no. de-sc0012311 (P.D.). A part of the materials work at Rice is supported by the Robert A. Welch Foundation Grants No. C-1839 (P.D.). The DFT calculation was partly supported by the National Natural Science Foundation of China (Grants No. 61604013) and the Fundamental Research Funds for the Central Universities (Grants No. 2016NT10).

* Electronic address: pdai@rice.edu

- [1] S. W. Lovesey, *Theory of Thermal Neutron Scattering from Condensed Matter* (Clarendon, Oxford, 1984), Vol. 2, Chap. 9.
- [2] L. D. Landau, *The Theory of a Fermi Liquid*, Sov. Phys. JETP **3**, 920 (1957).
- [3] M. E. Zhitomirsky and A. L. Chernyshev, *Colloquium: Spontaneous magnon decays*, Rev. Mod. Phys. **85**, 219 (2013).
- [4] Pengcheng Dai, *Antiferromagnetic order and spin dynamics in iron-based superconductors*, Rev. Mod. Phys. **87**, 855 (2015).
- [5] D. S. Inosov, *Spin fluctuations in iron pnictides and chalcogenides: From antiferromagnetism to superconductivity*, C. R. Phys. **17**, 60-89 (2016).
- [6] Jun Zhao, D. T. Adroja, Dao-Xin Yao, R. Bewley, Shiliang Li, X. F. Wang, G. Wu, X. H. Chen, Jiangping Hu, and Pengcheng Dai, *Spin waves and magnetic exchange interactions in CaFe_2As_2* , Nat. Phys. **5**, 555 (2009).
- [7] Joosung Oh, Manh Duc Le, Ho-Hyun Nahm, Hasung Sim, Jaehong Jeong, T.G. Perring, Hyungje Woo, Kenji Nakajima, Seiko Ohira-Kawamura, Zahra Yamani, Y. Yoshida, H. Eisaki, S.-W. Cheong, A.L. Chernyshev, and Je-Geun Park, *Spontaneous decays of magneto-elastic excitations in non-collinear antiferromagnet $(\text{Y,Lu})\text{MnO}_3$* , Nat. Commun. **7**, 13146 (2016).
- [8] Pengcheng Dai, H. Y. Hwang, Jiandi Zhang, J. A. Fernandez-Baca, S.-W. Cheong, C. Kloc, Y. Tomioka, and Y. Tokura, *Magnon damping by magnon-phonon coupling in manganese perovskites*, Phys. Rev. B **61**, 9553 (2000).
- [9] D. R. Parker, M. J. Pitcher, P. J. Baker, I. Franke, T. Lancaster, S. J. Blundell, and S. J. Clarke, *Structure, antiferromagnetism and superconductivity of the layered iron arsenide NaFeAs* , Chem. Commun. (Cambridge) 2189, (2009).
- [10] S. Li, C. de la Cruz, Q. Huang, G. F. Chen, T.-L. Xia, J. L. Luo, N. L. Wang, and Pengcheng Dai, *Structural and magnetic phase transitions in $\text{Na}_{1-\delta}\text{FeAs}$* , Phys. Rev. B **80**, 020504(R) (2009).
- [11] J. T. Park, G. Friemel, T. Loew, V. Hinkov, Yuan Li, B. H. Min, D. L. Sun, A. Ivanov, A. Piovano, C. T. Lin, B. Keimer, Y. S. Kwon, and D. S. Inosov, *Similar zone-center gaps in the low-energy spin-wave spectra of $\text{Na}_{1-\delta}\text{FeAs}$ and BaFe_2As_2* , Phys. Rev. B **86**, 024437 (2012).
- [12] J. D. Wright, T. Lancaster, I. Franke, A. J. Steele, J. S. Möller, M. J. Pitcher, A. J. Corkett, D. R. Parker, D. G. Free, F. L. Pratt, P. J. Baker, S. J. Clarke, and S. J. Blundell, *Gradual destruction of magnetism in the superconducting family $\text{NaFe}_{1-x}\text{Co}_x\text{As}$* , Phys. Rev. B **85**, 054503 (2012).
- [13] E. Fradkin, S. A. Kivelson, M. J. Lawler, J. P. Eisenstein, and A. P. Mackenzie, *Nematic Fermi Fluids in Condensed Matter Physics*, Annu. Rev. Condens. Matter Phys. **1**, 153 (2010).
- [14] C. Fang, H. Yao, W. Tsai, J. P. Hu, and S. A. Kivelson, *Theory of electron nematic order in LaFeAsO* , Phys. Rev. B **77**, 224509 (2008).
- [15] C. Xu, M. Muller, and S. Sachdev, *Ising and spin orders in the iron-based superconductors*, Phys. Rev. B **78**, 020501 (2008).
- [16] R. M. Fernandes, A. V. Chubukov, and J. Schmalian, *What drives nematic order in iron-based superconductors ?*, Nat. Phys. **10**, 97 (2014).
- [17] S. Liang, A. Moreo, and E. Dagotto, *Nematic State of Pnictides Stabilized by Interplay between Spin, Orbital, and Lattice Degrees of Freedom*, Phys. Rev. Lett. **111**, 047004 (2013).
- [18] I. R. Fisher, L. Degiorgi, and Z. X. Shen, *In-plane electronic anisotropy of underdoped '122' Fe-arsenide superconductors revealed by measurements of detwinned single crystals*, Rep. Prog. Phys. **74**, 124506 (2011).
- [19] H. -H. Kuo, J.-H., Chu, J. C. Palmstrom, S. A. Kivelson, and I. R. Fisher, *Ubiquitous signatures of nematic quantum criticality in optimally doped Fe-based superconductors*, Science **352**, 958 (2016).
- [20] Ming Yi, Donghui Lu, Jiun-Haw Chu, James G. Analytis, Adam P. Sorini, Alexander F. Kemper, Brian Moritz, Sung-Kwan Mo, Rob G. Moore, Makoto Hashimoto, Wei-Sheng Lee, Zahid Hussain, Thomas P. Devereaux, Ian R. Fisher, and Zhi-Xun Shen, *Symmetry-breaking orbital anisotropy observed for detwinned $\text{Ba}(\text{Fe}_{1-x}\text{Co}_x)_2\text{As}_2$ above the spin density wave transition*, Proc. Natl. Acad. Sci. U.S.A. **108**, 6878-6883 (2011).
- [21] Y. Zhang, C. He, Z. R. Ye, J. Jiang, F. Chen, M. Xu, Q. Q. Ge, B. P. Xie, J. Wei, M. Aeschlimann, X. Y. Cui, M. Shi, J. P. Hu, and D. L. Feng, *Symmetry breaking via orbital-dependent reconstruction of electronic structure in detwinned NaFeAs* , Phys. Rev. B **85**, 085121 (2012).
- [22] M. P. Allan, T.-M. Chuang, F. Masee, Yang Xie, Ni Ni, S. L. Bud'ko, G. S. Boebinger, Q. Wang, D. S. Dessau, P. C. Canfield, M. S. Golden, and J. C. Davis, *Anisotropic impurity states, quasiparticle scattering and nematic transport in underdoped $\text{Ca}(\text{Fe}_{1-x}\text{Co}_x)_2\text{As}_2$* , Nature Physics **9**, 220-224 (2013).
- [23] E. P. Rosenthal, E. F. Andrade, C. J. Arguello, R. M. Fernandes, L. Y. Xing, X. C. Wang, C. Q. Jin, A. J. Millis, A. N. Pasupathy, *Visualization of electron nematicity and unidirectional antiferroic fluctuations at high temperatures in NaFeAs* , Nature Physics **10**, 225- 232 (2014).
- [24] Xingye Lu, J.T. Park, Rui Zhang, Huiqian Luo, Andriy H. Nevidomskyy, Qimiao Si, and Pengcheng Dai, *Nematic spin correlations in the tetragonal state of uniaxial-strained $\text{BaFe}_{2-x}\text{Ni}_x\text{As}_2$* , Science (345), 657-660 (2014).
- [25] Qiang Zhang, Rafael M. Fernandes, Jagat Lamsal, Jiaqiang Yan, Songxue Chi, Gregory S. Tucker, Daniel K. Pratt, Jeffrey W. Lynn, R.W. McCallum, Paul C. Canfield, Thomas A. Lograsso, Alan I. Goldman, David Vaknin, and Robert J. McQueeney, *Neutron-Scattering Measurements of Spin Excitations in LaFeAsO and $\text{Ba}(\text{Fe}_{0.953}\text{Co}_{0.047})_2\text{As}_2$: Evidence for a Sharp Enhancement of Spin Fluctuations by Nematic Order*, Phys. Rev. Lett. **114**, 057001 (2015).
- [26] W. L. Zhang, J. T. Park, X. Y. Lu, Y. Wei, X. Y. Ma, L. J. Hao, P. C. Dai, Z. Y. Meng, Y.-f. Yang, H. Q. Luo, and S. L. Li, *Effect of Nematic Order on the Low-Energy Spin Fluctuations in Detwinned $\text{BaFe}_{1.935}\text{Ni}_{0.065}\text{As}_2$* , Phys. Rev. Lett.

- 117**, 227003 (2016).
- [27] M. A. Metlitski, D. F. Mross, S. Sachdev, and T. Senthil, *Cooper pairing in non-Fermi liquids*, Phys. Rev. B **91**, 115111 (2015).
- [28] S. Lederer, Y. Schattner, E. Berg, and S. A. Kivelson, *Enhancement of Superconductivity near a Nematic Quantum Critical Point*, Phys. Rev. Lett. **114**, 097001 (2015).
- [29] M. G. Cottam, *Spin-phonon interactions in a Heisenberg antiferromagnet. I. The spin-wave spectrum*, J. Phys. C: Solid State Phys. **7**, 2901 (1974).
- [30] M. G. Cottam, *Spin-phonon interactions in a Heisenberg antiferromagnet: II. The phonon spectrum and spin-lattice relaxation rate*, J. Phys. C: Solid State Phys. **7**, 2919 (1974).
- [31] F. Krüger, S. Kumar, J. Zaanen, and J. van den Brink, *Spin-orbital frustrations and anomalous metallic state in iron-pnictide superconductors*, Phys. Rev. B **79**, 054504 (2009).
- [32] W. Lv, J. Wu, and P. Phillips, *Orbital ordering induces structural phase transition and the resistivity anomaly in iron pnictides*, Phys. Rev. B **80**, 224506 (2009).
- [33] C.-C. Lee, W.-G. Yin, and W. Ku, *Ferro-Orbital Order and Strong Magnetic Anisotropy in the Parent Compounds of Iron-Pnictide Superconductors*, Phys. Rev. Lett. **103**, 267001 (2009).
- [34] H. Kontani and Y. Yamakawa, *Linear Response Theory for Shear Modulus C_{66} and Raman Quadrupole Susceptibility: Evidence for Nematic Orbital Fluctuations in Fe-based Superconductors*, Phys. Rev. Lett. **113**, 047001 (2014).
- [35] S.-H. Baek, D.V. Efremov, J.M. Ok, J.S. Kim, J. van den Brink, and B. Büchner, *Orbital-driven nematicity in FeSe*, Nat. Mater. **14**, 210-214 (2015).
- [36] A. E. Böhmer, T. Arai, F. Hardy, T. Hattori, T. Iye, T. Wolf, H.v. Lohneysen, K. Ishida, and C. Meingast, *Origin of the Tetragonal-to-Orthorhombic Phase Transition in FeSe: A Combined Thermodynamic and NMR Study of Nematicity*, Phys. Rev. Lett. **114**, 027001 (2015).
- [37] R. M. Fernandes, E. Abrahams, and J. Schmalian, *Anisotropic In-Plane Resistivity in the Nematic Phase of the Iron Pnictides*, Phys. Rev. Lett. **107**, 217002 (2011).
- [38] R. M. Fernandes and J. Schmalian, *Manifestations of nematic degrees of freedom in the magnetic, elastic, and superconducting properties of the iron pnictides*, Supercond. Sci. Technol. **25**, 084005 (2012).
- [39] A. E. Böhmer and C. Meingast, *Electronic nematic susceptibility of iron-based superconductors*, C. R. Phys. **17**, 90-112 (2016).
- [40] X. Y. Lu, K. F. Tseng, T. Keller, W.L. Zhang, D. Hu, Y. Song, H. Man, J. T. Park, H. Q. Luo, S. Li, A. H. Nevidomskyy, and P. C. Dai, *Impact of uniaxial pressure on structural and magnetic phase transitions in electron-doped iron pnictides*, Phys. Rev. B **93**, 134519 (2016).
- [41] Z. P. Yin, S. Lebegue, M.J. Han, B.P. Neal, S.Y. Savrasov, and W.E. Pickett, *Electron-Hole Symmetry and Magnetic Coupling in Antiferromagnetic LaFeAsO*, Phys. Rev. Lett. **101**, 047001 (2008).
- [42] I. I. Mazin and M.D. Johannes, *A key role for unusual spin dynamics in ferropnictides*, Nat. Phys. **5**, 141 (2009).
- [43] T. Yildirim, *Strong Coupling of the Fe-Spin State and the As-As Hybridization in Iron-Pnictide Superconductors from First-Principle Calculations*, Phys. Rev. Lett. **102**, 037003 (2009).
- [44] M. Zbiri, H. Schober, M. R. Johnson, S. Rols, R. Mittal, Y. X. Su, M. Rotter, and D. Johrendt, *Ab initio lattice dynamics simulations and inelastic neutron scattering spectra for studying phonons in BaFe₂As₂: Effect of structural phase transition, structural relaxation, and magnetic ordering*, Phys. Rev. B **79**, 064511 (2009).
- [45] S.E. Hahn, Y. Lee, N. Ni, P. C. Canfield, A.I. Coldman, R.J. McQueeney, B.N. Harmon, A. Alatas, B. M. Leu, E. E. Alp, D. Y. Chung, I. S. Todorov, and M. G. Kanatzidis, *Influence of magnetism on phonons in CaFe₂As₂ as seen via inelastic x-ray scattering* Phys. Rev. B **79**, 220511(R) (2009).
- [46] D. Reznik, K. Lokshin, D.C. Mitchell, D. Parshall, W. Dmowski, D. Lamago, R. Heid, K.-P. Bohnen, A.S. Sefat, M.A. McGuire, B.C. Sales, D.G. Mandrus, A. Subedi, D.J. Singh, A. Alatas, M.H. Upton, A.H. Said, A.Cunsolo, Yu. Shvyd'ko, and T. Egami, *Phonons in doped and undoped BaFe₂As₂ investigated by inelastic x-ray scattering*, Phys. Rev. B **80**, 214534 (2009).
- [47] Jennifer L. Niedziela, D. Parshall, K.A. Lokshin, A.S. Sefat, A. Alatas, and T. Egami, *Phonon softening near the structural transition in BaFe₂As₂ observed by inelastic x-ray scattering*, Phys. Rev. B **84**, 224305 (2011).
- [48] D. Parshall, L. Pintschovius, J.L. Niedziela, J.-P. Castellan, D. Lamago, R. Mittal, Th. Wolf, and D. Reznik, *Close correlation between magnetic properties and the soft phonon mode of the structural transition in BaFe₂As₂ and SrFe₂As₂*, Phys. Rev. B **91**, 134426 (2015).
- [49] F. Weber, D. Parshall, L. Pintschovius, J.-P. Castellan, M. Merz, Th. Wolf, and D. Reznik, *Finite-momentum nematic fluctuations soften phonons in the superconducting state of Ba(Fe_{1-x}Co_x)₂As₂*, arXiv: 1610.00099.
- [50] G. T. Tan, Y. Song, C. L. Zhang, L. F. Lin, Z. Xu, T. T. Hou, W. Tian, H. B. Cao, S. L. Li, S. P. Feng, and P. C. Dai, *Electron doping evolution of structural and antiferromagnetic phase transitions in NaFe_{1-x}Co_xAs iron pnictides*, Phys. Rev. B **94**, 014509 (2016).
- [51] See supplementary information for additional data and analysis.
- [52] R. M. Fernandes, L. H. VanBebber, S. Bhattacharya, P. Chandra, V. Keppens, D. Mandrus, M. A. McGuire, B. C. Sales, A. S. Sefat, and J. Schmalian, *Effects of Nematic Fluctuations on the Elastic Properties of Iron Arsenide Superconductor*, Phys. Rev. Lett. **105**, 157003 (2010).
- [53] Masahito Yoshizawa, Daichi Kimura, Taiji Chiba, Shalamujiang Simayi, Yoshiki Nakanishi, Kunihiro Kihou, Chul-Ho Lee, Akira Iyo, Hiroshi Eisaki, Masamichi Nakajima, and Shin-ichi Uchida, *Structural Quantum Criticality and Superconductivity in Iron-Based Superconductor Ba(Fe_{1-x}Co_x)₂As₂*, J. Phys. Soc. Jpn. **81**, 024604 (2012).
- [54] A. E. Böhmer, P. Burger, F. Hardy, T. Wolf, P. Schweiss, R. Fromknight, M. Reinecker, W. Schranz, and C. Mein-

- gast, *Nematic Susceptibility of Hole-Doped and Electron-Doped BaFe₂As₂ Iron-Based Superconductors from Shear Modulus Measurements*, Phys. Rev. Lett. **112**, 047001 (2014).
- [55] George Gruner, *Density Waves in Solids*, Cambridge, Mass.: Perseus Publishing, 2000.
- [56] Juanjuan Liu, Jinchun Wang, Wei Luo, Jieming Sheng, Aifeng Wang, Xianhui Chen, Sergey A. Danilkin, Wei Bao, *The influence of the structural transition on magnetic fluctuations in NaFeAs*, J.Phys.: Condens. Matter **28**, 27LT01 (2016).
- [57] C. L. Zhang, L. W. Harriger, Z. P. Yin, W. C. Lv, M. Y. Wang, G. T. Tan, Y. Song, D. L. Abernathy, W. Tian, T. Egami, K. Haule, G. Kotliar, and P. C. Dai, *Effect of Pnictogen Height on Spin Waves in Iron Pnictides*, Phys. Rev. Lett. **112**, 217202 (2014).
- [58] Since spin excitations in the paramagnetic tetragonal state is almost identical to those below T_s [62], the large differences in the effective magnetic exchange couplings along the orthorhombic a_o and b_o directions within the Heisenberg Hamiltonian cannot be due to the small lattice parameter differences below T_s . Due to the strong spin-lattice coupling, the biquadratic interaction $-K(\mathbf{S}_i \cdot \mathbf{S}_j)^2$ between the nearest-neighbor spins becomes important and can therefore account for the large differences in SJ_{1a} and SJ_{1b} in the Heisenberg Hamiltonian. See, for example, A. L. Wysocki, K. D. Belashchenko, and V. P. Antropov, Nat. Phys. **7**, 485 (2011) and R. Yu, Z. T. Wang, P. Goswami, A. H. Nevidomskyy, Q. Si, and E. Abrahams, Phys. Rev. B **86**, 085148 (2012). Therefore, our discussion here only serves to illustrate the need for dynamic spin-lattice coupling below and above T_s , and the Heisenberg Hamiltonian by itself is insufficient to describe the data.
- [59] K.W. Kim, A. Pashkin, H. Schafer, M. Beyer, M. Porer, T. Wolf, C. Bernhard, J. Demsar, R. Huber, and A. Leitenstorfer, *Ultrafast transient generation of spin-density-wave order in the normal state of BaFe₂As₂ driven by coherent lattice vibrations*, Nat. Mater. **11**, 497-501 (2012).
- [60] Aaron Patz, Tianqi Li, Sheng Ran, Rafael M. Fernandes, Joerg Schmalian, Sergey L. Bud'ko, Paul C. Canfield, Ilias E. Perakis, and Jigang Wang, *Ultrafast observation of critical nematic fluctuations and giant magnetoelastic coupling in iron pnictides*, Nat. Commun. **5**, 3229 (2014).
- [61] Z. J. Xiong, T. Datta, K. Stiwinter, and D. X. Yao, *Magnon-phonon coupling effects on the indirect \mathbf{K} -edge resonant inelastic x-ray scattering spectrum of a two-dimensional Heisenberg antiferromagnet*, Phys. Rev. B **96**, 144436 (2017).
- [62] Leland W. Harriger, Mengshu Liu, Huiqian Luo, R.A. Ewings, C.D. Frost, T.G. Perring, and Pengcheng Dai, *Temperature dependence of the paramagnetic spin excitations in BaFe₂As₂*, Phys. Rev. B **86**, 140403(R) (2012).
- [63] G. S. Dixon, *Lattice thermal conductivity of antiferromagnetic insulators*, Phys. Rev. B **21**, 2851 (1980).
- [64] In Fig. 2, the maximum of the softening occurring around $q = 0.05$ gives a characteristic energy scale of ~ 1 meV.